Time-varying parameter identification of bridges subject to moving vehicles using ridge extraction based on empirical wavelet transform

Jiantao Li[a,b] , Jian Guo[a,*] and Xinqun Zhu[b]

[a] Institute of Bridge Engineering, Zhejiang University of Technology, Hangzhou 310000, Zhejiang, China. Email: Guoj@zjut.edu.cn

[b] School of Civil and Environmental Engineering, University of Technology Sydney, Broadway, NSW 2007, Australia

Abstract

When a vehicle moves over the bridge, the vehicle-bridge interaction(VBI) leads to the time-varying modal parameters of the system. The identification of non-stationary characteristics of bridge responses due to moving vehicle load is important and remains a challenging task. A new method based on the improved empirical wavelet transform (EWT) along with ridge detection of signals in time-frequency representation (TFR) is proposed to estimate the instantaneous frequencies (IFs). Numerical studies are conducted using a vehicle-bridge interaction model to investigate the time-varying characteristics of the system. The effects of the measurement noise, road surface roughness and structural damage, on the bridge IFs are investigated. Finally, the dynamic responses of an in-situ cable-stayed bridge subjected to a passing vehicle are analyzed to further explore the time varying characteristics of the VBI system. Numerical and experimental studies demonstrate the feasibility and effectiveness of the proposed method on the IF estimation. The identified IFs reveal important time-varying characteristics of the bridge dynamic that is significant to evaluate the actual performance of operational bridge and may be used for the structural health assessment.

Keywords: vehicle-bridge interaction, instantaneous modal frequencies, empirical wavelet transform, time-frequency representation, ridge detection

1. Introduction

The investigation on the bridge dynamic characteristics under operational traffic load is a significant part of the bridge structural health monitoring. Extensive study on the bridge dynamic characteristics has been conducted in a VBI framework[1-4]. Research shows that the VBI is a time-varying process that the dynamic responses of the bridge are non-stationary[5,6]. Li et al.[7] theoretically studied the natural frequency of railway girder bridges under vehicular load. The bridge frequency was found varying periodically with the passage of the vehicle. Kim et al.[8] experimentally studied the effect of vehicle weight on the bridge natural frequencies under traffic-induced excitation. A non-negligible change 5.4% was noted in the natural frequencies of a short span bridge when the mass ratio between the vehicle and the bridge was 3.8%. Chang et al.[9] conducted theoretical and experimental studies to estimate the variability of bridge frequency due to a vehicle parked on top. Cantero et al.[10] assessed the non-stationary and non-linear features of a scaled vehicle-bridge interaction test bed experimentally. The identification of the time-varying dynamic characteristics is critical to accurately assess the structural performance and condition of target structure[11]. The time-varying parameter identification of bridges under moving vehicle loads is still a big challenge.

Non-parametric based time-frequency analysis techniques, i.e. short time Fourier transform (STFT), Winger-Ville distribution (WVD), Empirical Mode Decomposition (EMD) and wavelet transform, are extensively used to study dynamic characteristics of nonstationary structural responses[12,13]. Yang *et al.*[14] briefly reviewed these methods and their engineering applications. For fixed-window STFT, the obtained

time-frequency are determined by the window function and the resolutions are fixed that may fail to extract high accuracy time-frequency characteristics from nonstationary signals. The time-frequency representation based on continuous wavelet transform is a trade-off between time-frequency resolutions, while the results of WVD are affected by the cross-terms in the instantaneous auto-correlation function. EMD and the ensemble EMD become one of the most popular techniques to analyze non-stationary and non-linear dynamic response signals. It decomposes a signal into a finite sum of Intrinsic Mode Functions (IMFs) and Hilbert transform (HT) is used to extract the instantaneous modal frequencies from IMFs. However, the main issue of the EMD approach is its lack of mathematical theory. The EMD suffers from the problems of mode mixture and pseudo-IMFs, etc. The synchrosqueezing transform (SST), an EMD-like tool, was recently proposed to analyze the non-stationary signals[15,16]. SST based methods have been developed for the time-frequency analysis and IF estimation and presents better estimation results over EMD[17,18]. However, the SST method was a smart utilization of the output of a classic wavelet analysis instead of a full adaptive wavelet transform.

Gills[19] developed the Empirical Wavelet Transform (EWT) based on wavelet decomposition. EWT is an adaptive approach for conveniently extracting the different modes of a signal by constructing a wavelet filter bank. The results have shown the its feasibility and effectiveness compared to the classic EMD. It has been successfully applied to machinery fault diagnosis[20-22]. Kedadouche *et al.*[23] compared the EWT and EMD methods in the application to the bearing effect diagnosis. The results showed that the EWT was much efficient compared to EMD and Ensemble EMD on mode estimates and computation time. Recently, EWT was applied to identify modal parameters of civil structures[24]. Xia and Zhou[25] adopted EWT to obtain the mono-component of structural response and employed Hilbert transform to extract the time-varying features for condition assessment of civil structures. The EWT approach is to extract the different modes by designing the appropriate wavelet filter bank and provides a consistent decomposition. To authors' best knowledge, there is a little research on using or improving EWT method for time-varying parameter identification, especially for vehicle-bridge interaction systems. Xin et al.[26] proposed an improved EWT approach for structural operational modal identification. The Fourier spectrum was replaced with a standardized autoregression (AR) power spectrum to determine the spectrum boundaries associated with EWT analysis. Hilbert transform and RDT were then performed to identify the structural modal parameters. The approach has been successfully applied for operational modal identification of linear structures. This method is enhanced using the time-frequency analysis based on Synchroextracting transform to determine the filtering boundaries of EWT [27]. The results showed that the EWT is more reliable and accurate to identify the time-varying components of the signal than that by the variational mode decomposition [28]. The experimental results showed the potential application to track the passage of the heavy vehicles on the bridge [27]. There is no detail study for time-varying characteristics of bridges subjected moving vehicles.

This paper proposes a hybrid framework based on an improved EWT for the analysis of non-stationary bridge responses under operational vehicle load and extract instantaneous frequencies. Two steps are involved in the framework. In the first step, an improved EWT is used to decompose the measured bridge responses into a number of IMFs. The second step is to extract instantaneous frequencies from the time-frequency represents (TFR) of IMFs by ridge detection. The rest of this paper is organized as follows: Section 2 presents the formulation of the 2-D VBI model for analysis and road surface roughness is included. In Section 3, the background of the EWT is brief introduced and the proposed hybrid method for the estimation of time-dependent characteristic is described. Section 4

conducts numerical analysis on the estimation of instantaneous modal frequencies to verify the feasibility of proposed framework. Experimental analysis on an actual cable-stayed bridge are conducted in Section 5. Section 6 summaries the conclusions.

2. Formulation of the VBI model

2.1 Equation of motion of a bridge subjected to a moving vehicle

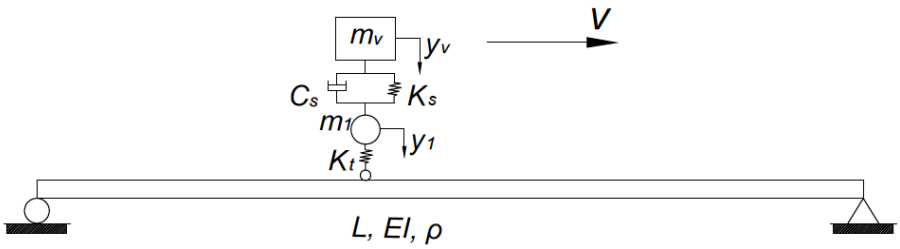

Figure 1 Vehicle-bridge interaction model

A VBI model as shown in Figure 1 is considered. The vehicle is modelled as a 2-DoF quarter car and the bridge as a simply-supported beam with length *L*. The vehicle parameters m_v and m_1 are the masses of vehicle body and axle, respectively. k_s and c_s are the stiffness and damping of suspension spring and damper, respectively. k_t is the stiffness of the tire. The vehicle is assumed to move along the bridge deck at a constant velocity *v*. The equation of motion for the vehicle can be expressed as

$$\begin{bmatrix} m_v & 0 \\ 0 & m_1 \end{bmatrix} \begin{Bmatrix} \ddot{y}_v \\ \ddot{y}_1 \end{Bmatrix} + \begin{bmatrix} c_s & -c_s \\ -c_s & c_s \end{bmatrix} \begin{Bmatrix} \dot{y}_v \\ \dot{y}_1 \end{Bmatrix} + \begin{bmatrix} k_s & -k_s \\ -k_s & k_s \end{bmatrix} \begin{Bmatrix} y_v \\ y_1 \end{Bmatrix} = \begin{Bmatrix} 0 \\ (m_v + m_1)\mathrm{g} - P_{int}(t) \end{Bmatrix} \quad (1)$$

where y_v and y_1 are the displacement responses of the vehicle body and axle, respectively. The interaction force between the bridge and the vehicle $P_{int}(t) = (m_v + m_1)\mathrm{g} + k_t(y_1 - y(x(t)) - r(x(t)))$. $y(x(t))$ is the displacement response of the bridge, and $r(x(t))$ is the road surface roughness of the bridge deck at the location $x(t) = vt$. Eq. (1) is rewritten as

$$\mathbf{M}_v\ddot{\mathbf{d}}_v(t) + \mathbf{C}_v\dot{\mathbf{d}}_v(t) + \mathbf{K}_v\mathbf{d}_v(t) = \mathbf{D}(F_v - P_{int}) \quad (2)$$

As shown in Figure 1, the planar Euler-Bernoulli beam bridge can be modelled with *n* finite elements. The equation of motion of the bridge can be expressed as[28]:

$$\mathbf{M}_b\ddot{\mathbf{d}}_b(t) + \mathbf{C}_b\dot{\mathbf{d}}_b(t) + \mathbf{K}_b\mathbf{d}_b(t) = \mathbf{H}_c(t)P_{int}(t) \quad (3)$$

where $\mathbf{d}_b$ denotes the vertical displacement vector of the bridge. $\mathbf{M}_b$, $\mathbf{C}_b$, $\mathbf{K}_b$ are the mass, damping and stiffness matrices of the bridge, respectively. $\mathbf{H}_c(t) = \{0, 0 \dots, \boldsymbol{H}_i(t), \dots, 0\}^T$ is a function of time and $\boldsymbol{H}_i(t)$ is the vector of shape function in the *ith* element on which the moving vehicle is located at time instant *t*, and it can be expressed as $\boldsymbol{H}_i(t) = \{1 - 3\xi^2 + 2\xi, (\xi - 2\xi^2 + \xi^3)l_e, 3\xi^2 - 2\xi^3, (-\xi^2 + \xi^3)l_e\}$, with $\xi = (x(t) - x_i)/l_e$, $x_i = (i-1)l_e$ where l_e is the length of the element.

Combining Eqs. (2) and (3), the coupled VBI system can be obtained as

$$\mathbf{M}\ddot{\boldsymbol{D}}(t) + \mathbf{C}\dot{\boldsymbol{D}}(t) + \mathbf{K}\boldsymbol{D}(t) = \mathbf{F}(t) \quad (4)$$

where $\boldsymbol{D}(t) = \begin{Bmatrix} \mathbf{d}_b(t) \\ y_v \\ y_1 \end{Bmatrix}$, $\mathbf{M} = \begin{bmatrix} \mathbf{M}_b & \mathbf{H}_c(t)m_v & \mathbf{H}_c(t)m_1 \\ 0 & m_v & 0 \\ 0 & 0 & m_1 \end{bmatrix}$, $\mathbf{C} = \begin{bmatrix} \mathbf{C}_b & 0 & 0 \\ 0 & c_s & -c_s \\ 0 & -c_s & c_s \end{bmatrix}$, $\mathbf{K} = \begin{bmatrix} \mathbf{K}_b & 0 & 0 \\ 0 & k_s & -k_s \\ -\mathbf{H}_c^T(t)k_t & -k_s & k_s + k_t \end{bmatrix}$, $\mathbf{F}(t) = \begin{Bmatrix} \mathbf{H}_c(t)(m_v + m_1)\mathrm{g} \\ 0 \\ k_t r(x(t)) \end{Bmatrix}$. The system matrices of the coupled interaction system in Eq. (4) are noted time-dependent according to the location of the interacting force

and the frequencies of the system is time-varying.

3. Theoretical background of the hybrid analysis method for IF estimations

3.1 The empirical wavelet transform

A dynamic response signal of a bridge $s(t)$ can be assumed to consist of *N* mono-components $\{s_i(t), i = 1,2, \dots, N)\}$, which correspond to modes centered on a specific frequency of the spectrum. The EWT separate the different modes mainly in three steps. First, the frequency spectrum of the signal $s(t)$ is obtained with the frequency rang $[0,\ \pi]$ by using Fourier transform. Second, the spectrum along the Fourier axis is segmented into *N* number of contiguous portions according to the local maxima of spectrum. The individual segments correspond to different modes that are centered around each local maximum.

The boundary between each segment is denoted as ω_n and each segment is filtered by an interval $[\omega_{n-1},\ \omega_n]$ with $(\omega_0 = 0 \text{ and } \omega_N = \pi)$. A transition phase T_n of width $2\,\tau_n$ is defined for each ω_n. The τ_n can be defined as

$$\tau_n = \gamma\omega_n \tag{5}$$

and γ is chosen by $0 < \gamma < \min_n \frac{\omega_{n+1}-\omega_n}{\omega_{n+1}+\omega_n}$. At last, the filter bank for each segment is defined by the empirical scaling function and the empirical wavelets expressed as:

$$\hat{\phi}_n(\omega) = \begin{cases} 1 & \text{if } |\omega| \le (1-\gamma)\omega_n \\ \cos\left[\frac{\pi}{2}\beta\left(\frac{1}{2\gamma\omega_n}(|\omega| - (1-\gamma)\omega_n)\right)\right] & \text{if } (1-\gamma)\omega_n \le |\omega| \le (1+\gamma)\omega_n \\ 0 & \text{otherwise,} \end{cases} \tag{6}$$

$$\hat{\psi}_n(\omega) = \begin{cases} 1 & \text{if } (1+\gamma)\omega_n \le |\omega| \le (1-\gamma)\omega_{n+1} \\ \cos\left[\frac{\pi}{2}\beta\left(\frac{1}{2\gamma\omega_{n+1}}(|\omega| - (1-\gamma)\omega_{n+1})\right)\right] & \text{if } (1-\gamma)\omega_{n+1} \le |\omega| \le (1+\gamma)\omega_{n+1} \\ \sin\left[\frac{\pi}{2}\beta\left(\frac{1}{2\gamma\omega_n}(|\omega| - (1-\gamma)\omega_n)\right)\right] & \text{if } (1-\gamma)\omega_n \le |\omega| \le (1+\gamma)\omega_n \\ 0 & \text{otherwise.} \end{cases} \tag{7}$$

in which the function $\beta(x)$ is an arbitrary function defined on [0,1] that can be expressed as

$$\beta(x) = \begin{cases} 0 & \text{if } x \le 0 \\ \beta(x) + \beta(1-x) = 1 & \forall x \in [0,1] \\ 1 & \text{if } x \ge 1 \end{cases} \tag{8}$$

and the most used one in the literatures[19,29] is:

$$\beta(x) = x^4(35 - 84x + 70x^2 - 20x^3) \tag{9}$$

After the scaling function and empirical wavelets are derived, the detail coefficients are given by the inner products with the empirical wavelets $\hat{\psi}_n$:

$$W_s(n,t) = \langle s(t), \hat{\psi}_n \rangle = \left(s(\omega)\overline{\hat{\psi}_n(\omega)}\right)^{\vee} \tag{10}$$

and the approximation coefficients are given by the inner product with the scaling function:

$$W_s(0,t) = \langle s(t), \hat{\phi}_1 \rangle = \left(s(\omega)\overline{\hat{\phi}_1(\omega)}\right)^{\vee} \tag{11}$$

where $\overline{\cdot}$ denotes the complex conjugate, $(.)^{\vee}$ denotes the inverse Fourier transform, and $\langle .,. \rangle$ denotes the inner product.

The empirical mode s_n is given by

$$s_0(t) = W_s(0,t) * \phi_1(t) \tag{12a}$$

$$s_n(t) = W_s(n,t) * \psi_n(t) \tag{12b}$$

where $*$ denotes a convolution.

3.2 The improved EWT approach

Using Fourier spectrum for determining the boundaries associated with EWT analysis of noisy and nonstationary signals may be challenging or lead to false modes[26]. The AR power spectrum is smoothed with a lower level variance compared with Fourier spectrum. So, it can better define the boundaries of EWT than using Fourier spectrum. Therefore, the AR power spectrum is employed to improve the effectiveness in defining the boundaries for using EWT to perform the signal decomposition. The most common form of parametric spectral density estimate uses an autoregressive model AR(p) of order p. The signal sequence $s(t)$ obeying a zero mean AR(p) process can be expressed as[30]:

$$s(t) = \phi_1 s(t-1) + \phi_2 s(t-2) + \cdots + \phi_p s(t-p) + \epsilon(t) \tag{13}$$

where p denotes the order of the AR model; the $\phi_1, \ldots, \phi_p$ are the model coefficients and $\epsilon(t)$ is a white noise process with zero mean and innovation variance σ_p^2. The power spectrum of the process $P_{AR}(e^{jw})$ is

$$P_{AR}(e^{jw}) = \frac{\sigma_p^2}{\left|1 - \sum_{k=1}^{p} \phi_k e^{-jwk}\right|^2} \tag{14}$$

There are a number of approaches to determine the order q, i.e., Singular Value Decomposition, Akaika Information Criterion, and Final Prediction Error Criterion[31]. The Akaike's Final Prediction Error is used to get the optimal q of AR model. When the optimal order is identified, the model parameters and thus the spectral density can be estimated. The Burg algorithm is used to calculate the AR power spectrum in this study.

3.3 IFs estimation of the decomposed modes

Once the component is extracted by EWT, the instantaneous frequency can be estimated. In this study, the technique for the extraction of IFs from ridges in TFR of signals[32] is adopted. First, wavelet transform (WT) is used to obtain the time-frequency representation of the response component[33], and the obtained TFR is $H_s(\omega, t)$. Second, the fast path optimization approach employing a support function is developed to optimally extract the ridge of the TFR corresponding to the IFs. If the ridge frequencies at each time is denoted as $v_m(t)$, TFR amplitudes as $Q_m(t)$, and their numbers as $N_p(t)$, the following relation can be obtained:

$$v_m(t): \begin{cases} [\partial_\omega |H_s(\omega,t)|]_{\omega = v_m(t)} = 0, \\ [\partial_\omega^2 |H_s(\omega,t)|]_{\omega = v_m(t)} < 0, \end{cases} \tag{15a}$$

$$Q_m(t) \equiv |H_s(v_m(t), t)| \tag{15b}$$

Since the $H_s(\omega, t)$ has a time span $t_n = (n-1)\Delta t$ for $n = 1, \ldots, N$, the path optimization can be described as

$$\{m_c(t_1), \ldots, m_c(t_N)\} = \underset{\{m_1 \ldots, m_N\}}{\arg\max} \; F[t_n, Q_m(t_n), v_m(t_n), \{v_{m1}(t_1), \ldots, v_{mN}(t_N)\}] \tag{16}$$

where $m_c(t_n)$ is the sequence of peak indices to be extracted as the ridge at t_n, and F is the chosen support function for the optimization. Last, an adaptive support function is constructed, and the optimization problem is solved with the fast path optimization. The detailed procedure of the scheme can be referred to literature[32,34].

Based on the above analysis procedures, the flowchart of the proposed IF estimation method is shown in Figure 2.

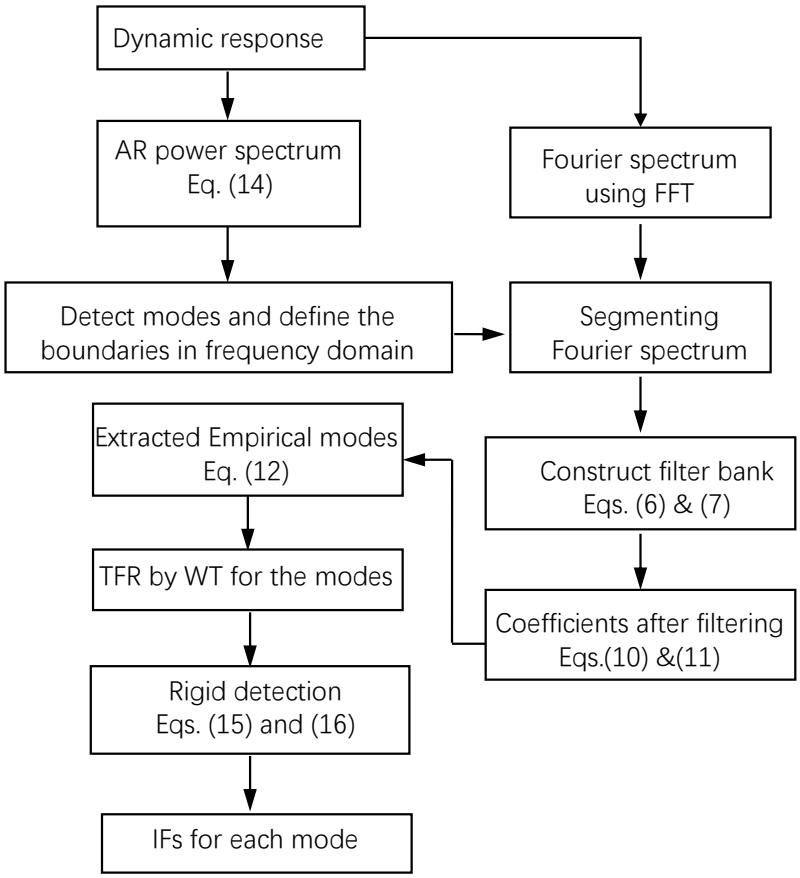

Figure 2. Flowchart of the IF estimation approach

4. Numerical study on time-varying parameter identification of the bridge subject to a moving vehicular load

The VBI system as shown in Figure 1 is studied. The select properties of the bridge are: $L = 30\text{m}, \rho = 6000\,\text{kg/m}$, $EI = 2.3e10\text{Nm}$. Rayleigh damping is assumed with $\mathbf{C}_b=\alpha_1\mathbf{M}_b+\alpha_2\mathbf{K}_b$ and $\alpha_1=0.344$, $\alpha_2=0.0002$, where $\mathbf{M}_b$, $\mathbf{C}_b$ and $\mathbf{K}_b$ are the mass, damping and stiffness matrices of the bridge respectively. The first three theoretical bridge modal frequencies are 3.42, 13.68 and 30.77Hz, respectively.

4.1 Moving mass case

A vehicle moving over the bridge is simplified as a moving mass in this case. The mass can be viewed as extra weight to the bridge system that would change the mass property of the bridge structure. Since the location of the extra mass on the bridge is time varying, the physical property of the bridge system is also time dependent. As a result, the modal frequencies of the bridge system, are time varying. Therefore, the IFs, instead of the fixed modal frequencies, are more suitable to describe the operational dynamic performance of the bridge system. A mass of 6000kg is assumed to move over the bridge with a speed of 5m/s. The dynamic response measured at the 3/8 span of the bridge is analyzed using the proposed method to get the IFs under the moving mass. Figure 3(a) shows the AR spectrum of the signal and the identified boundaries. The first three bridge modal frequencies are identified. The EWT is used to decompose the response and the obtained three modes corresponding to the bridge vibration are shown in Figure 3(b). The TFR of each mode is calculated and the 3-dimensional plotting of the results are

shown in Figure 4. The final results of the analysis are the ridge point of the TFR in Figure 4 corresponding to the IFs of bridge vibration mode. In order to evaluate the accuracy of the proposed method on the identification, the identified IFs are compared to the theoretical values which are obtained via eigenvalue analysis of $M^{-1}K$. M and K are the mass and stiffness matrices in Eq. (4), respectively. The damping has not been considered in the theoretical values. The comparison of the results is given in Figure 5. It can be seen that the variation trend of the frequencies identified are consistent to the theoretical values. The IF of the first vibration mode identified using the proposed method are very close to the theoretical values. The obvious difference at the beginning and the end of the results are due to the very small dynamic amplitude of the bridge when the mass is close to the supports and the end effect of the TFR. The values of the second and third modes are a bit smaller than the theoretical values. This is due to the damping has not been considered in the theoretical values. The identified results using the proposed method are obtained from the bridge responses based on Eq. (4) and the damping is included. Besides, some local fluctuations of the IFs are observed for those two modes. The reason can be due to that the system frequencies is modulated by the driving frequency $n\frac{\pi v}{L}$, where n is the mode order, v is the moving speed of vehicle and L is the bridge length[37].

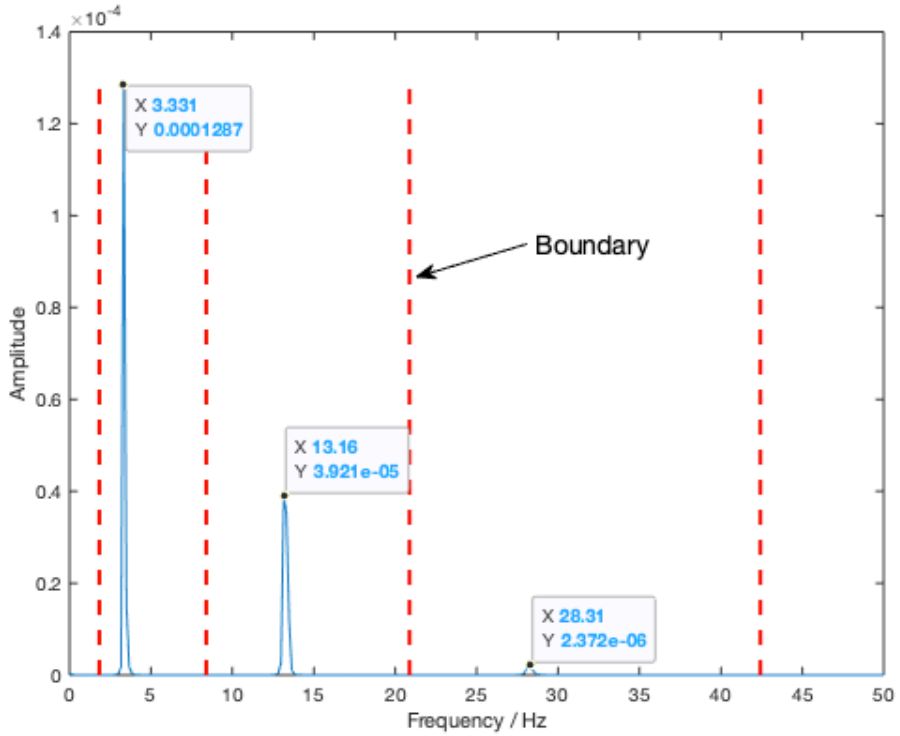

(a) The obtained AR spectrum and identified boundaries

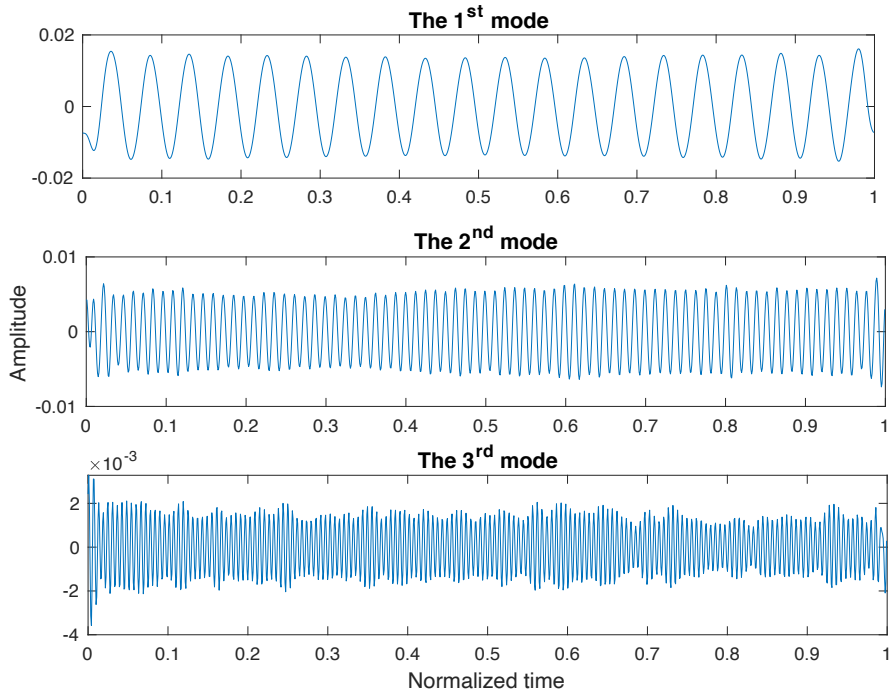

(b) Extracted first three components

Figure 3 Application of the improved EWT

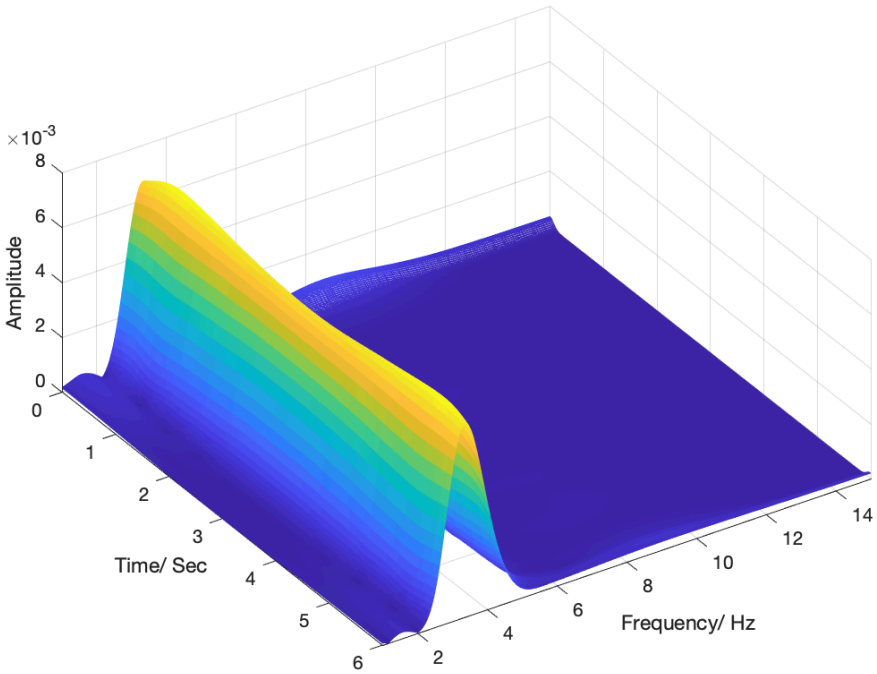

(a) TFR of 1st mode

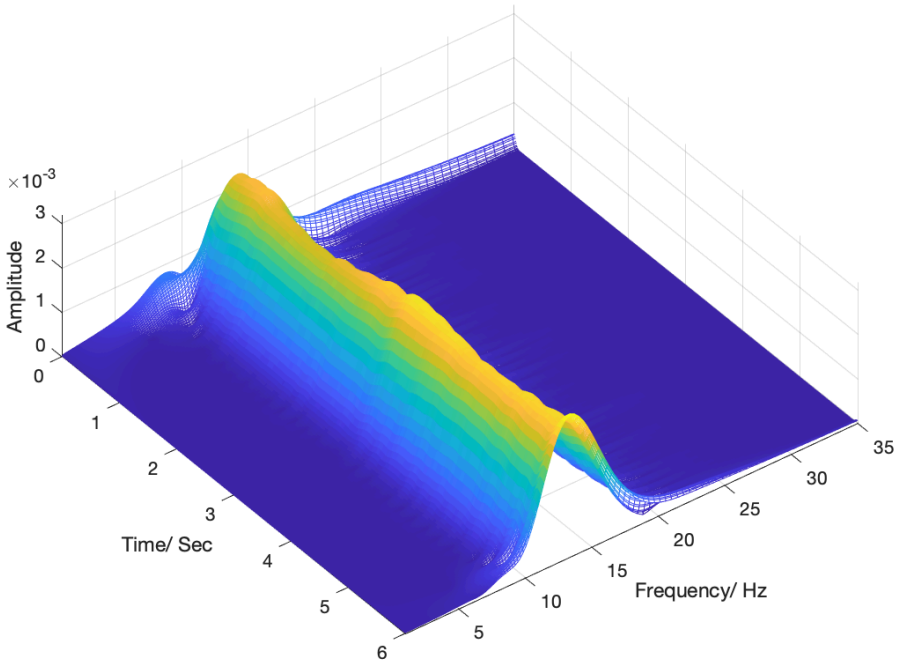

(b) TFR of 2nd mode

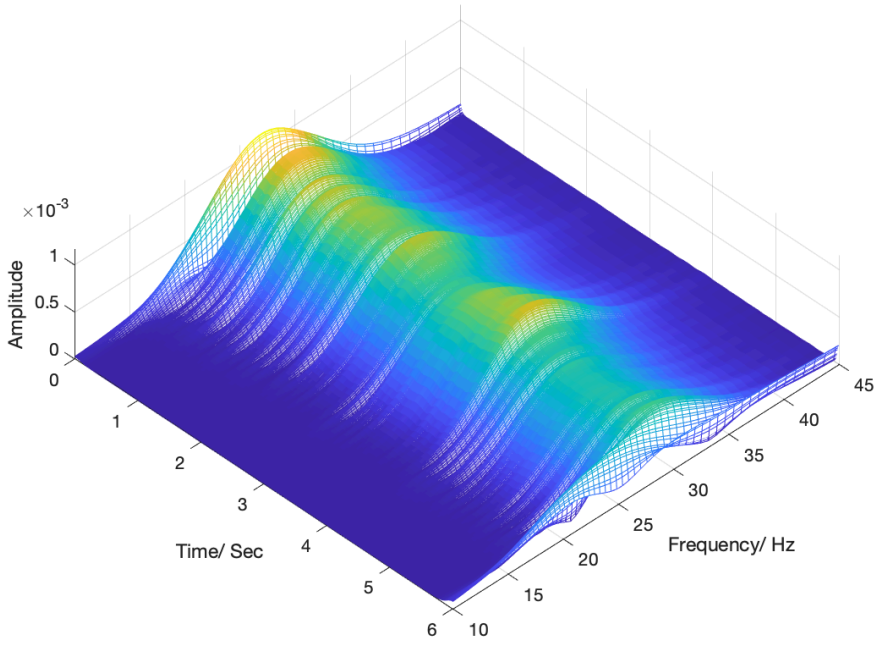

(c) TFR of 3rd mode

Figure 4 TFR of obtained vibration mode

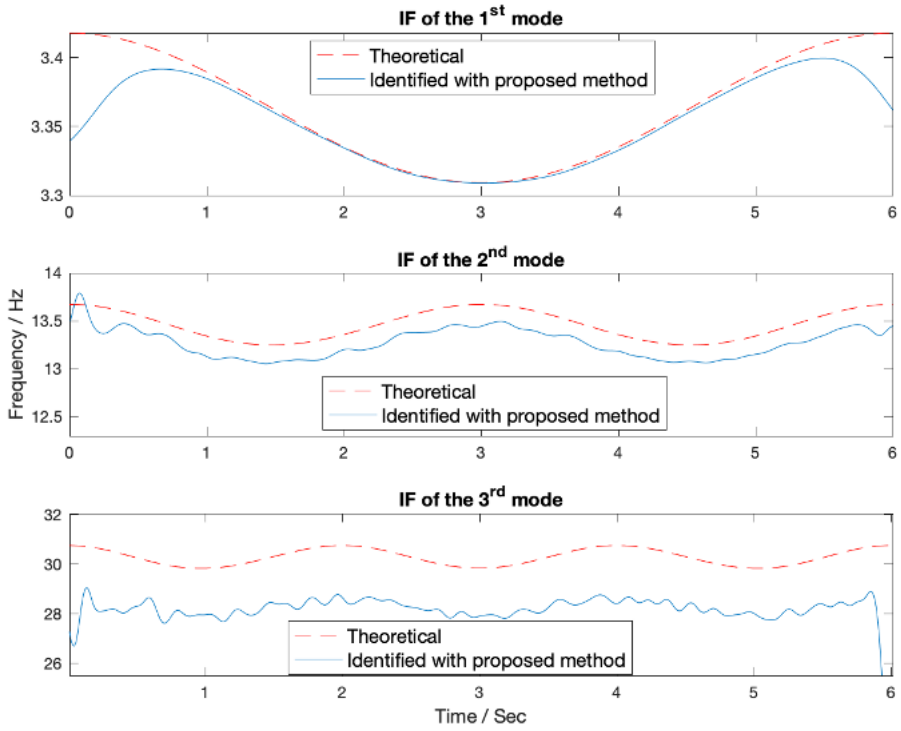

Figure 5 Comparison between the identified IFs and theoretical values

4.2 Moving vehicle case

For more practical study, a vehicle model with parameters $m_v = 4500\text{kg}$, $m_1 = 1500\text{kg}$, $k_t = 2.00e4\text{N/m}$, $k_s = 5e5\text{N/m}$ and $c_s = 5000\ \text{N/m/s}$ is adopted. The bounce frequency of vehicle body vibration is 0.33Hz and 2.96Hz is for the axle mass vibration. The moving speed is 10m/s with sampling frequency 200Hz. The dynamic response of the bridge is calculated using Newmark-ß method and 10% white noise is added to simulate the measurement. The dynamic measurement is simulated as follows,

4.2.1 Comparison of IF estimation using different methods

The dynamic response of the bridge under a moving vehicle is analyzed when the bridge road surface is smooth. The instantaneous frequencies are extracted from the bridge response using the proposed method and compared with that by SST and HT. Figure 6 shows the signal decomposition results using EWT. In Figure 6(a), three dominant peaks in the spectrum are corresponding to the bridge modal frequencies, while the vehicle-related frequency is invisible. The local maxima in the spectrum can successfully detect the boundary. The signal is decomposed by EWT and the bridge dynamic related three components are extracted as shown in Figure 6(b). The IFs identified for the moving vehicle case are shown in Figure 7 and the results are compared with those of moving mass case. It can be seen that the amplitude of bridge frequency variation under moving vehicle is smaller than that of moving mass. Figure 8 compares the identified IFs using the proposed method with that by SST and HT. For comparison, only the identified 1st and 2nd bridge modal frequencies are presented in Figure 8. From the results, it can be seen that the identified IFs from three different methods present a similar variation trend

and the proposed method outperforms the other two methods in regarding to the resolution. The rest of the study focuses on the identified IFs results.

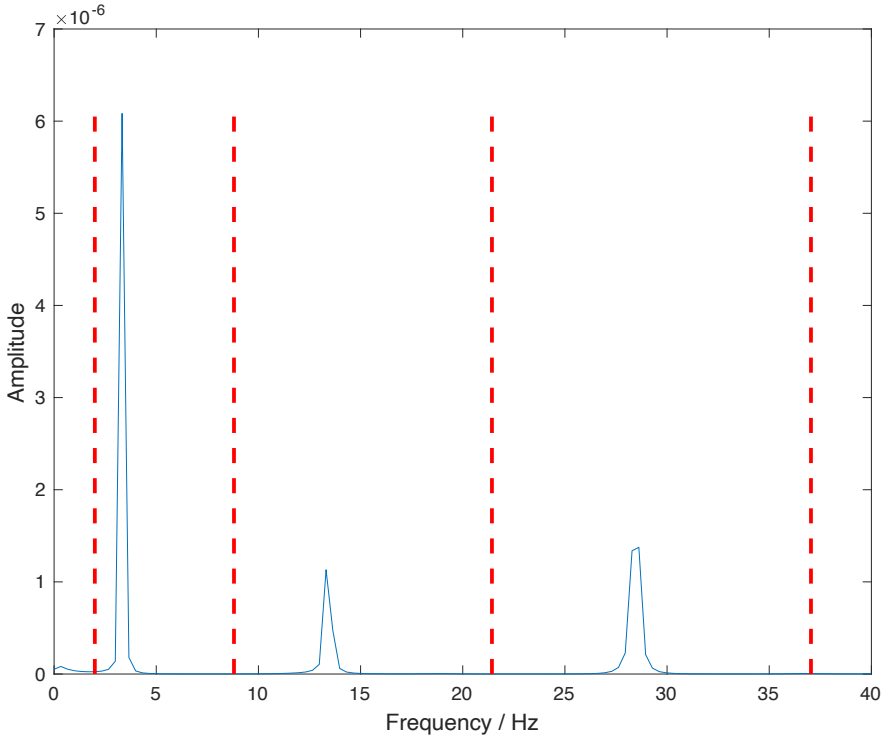

(a) Spectrum of the response and identified boundaries

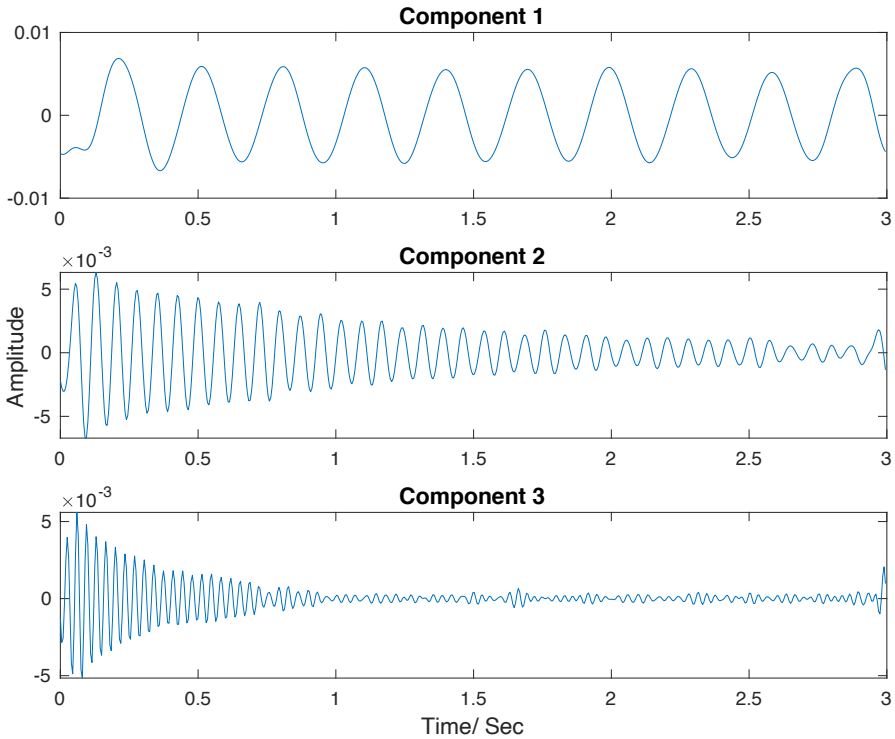

(b) First three components

Figure 6 Signal decomposition using EWT

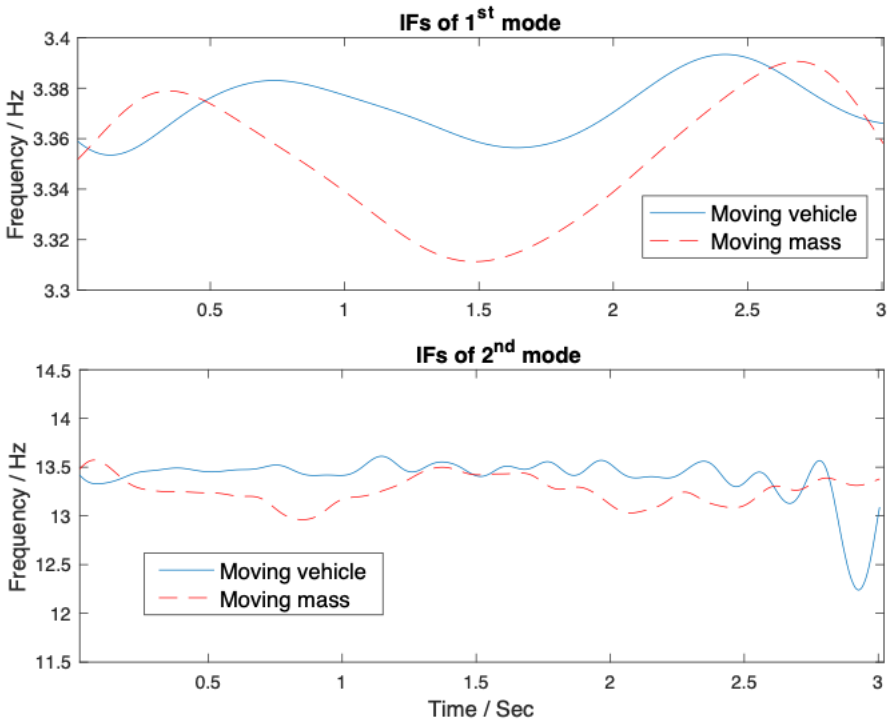

Figure 7 Signal decomposition using EWT

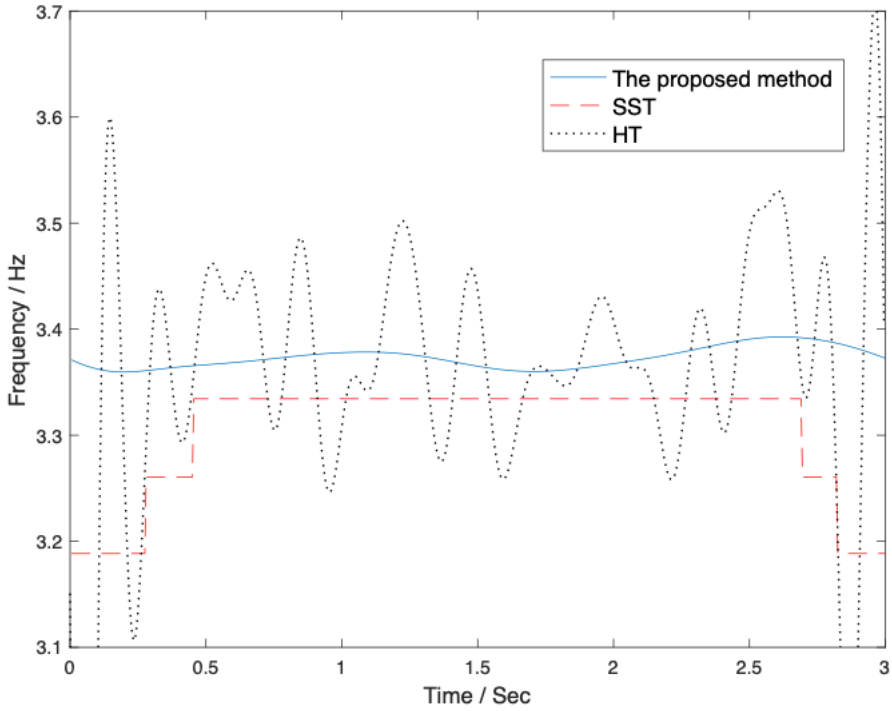

(a) IFs of first mode

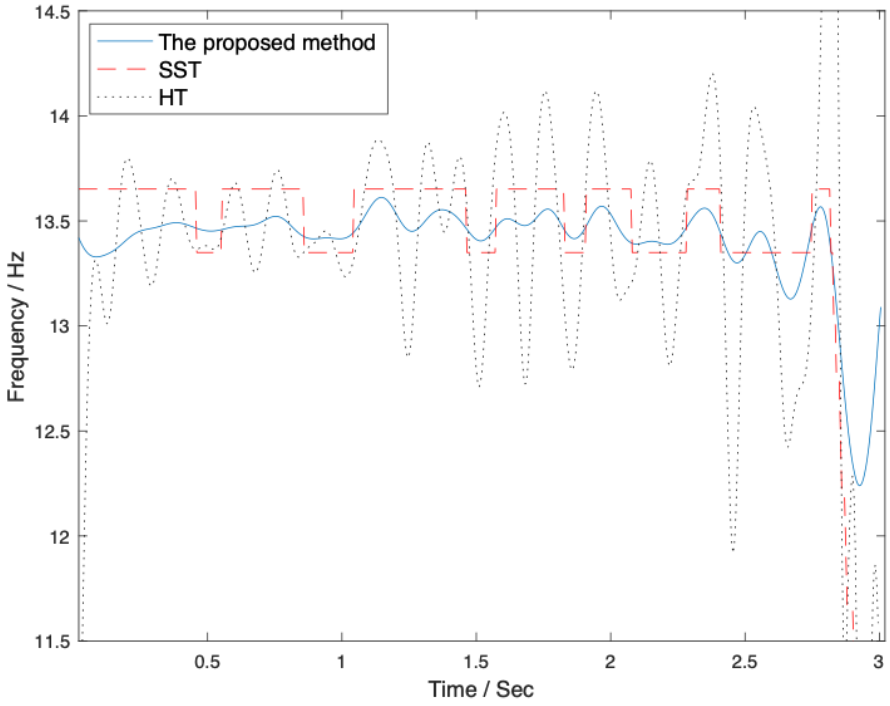

(b) IFs of second mode

Figure 8 Estimated IFs of bridge response using three different methods

4.2.2 Effect of measurement noise

The effects of measurement noise on the identification of the IFs using the proposed method are studied. Another two additional noise levels, i.e. 15% and 20% are included to the calculated bridge responses. The IF trajectories identified from the responses are given in Figure 9. In this figure, it can be seen that the identified IF trajectories related to vehicle frequency and 1st bridge modal frequency are very close for different noise levels. For the IF trajectory of the 2nd bridge modal frequency, there is an obvious difference in the identified results. The difference can be due to the effect of the driving frequency. Thus, the modal frequency of higher modes may present higher difference due to the effect of noise.

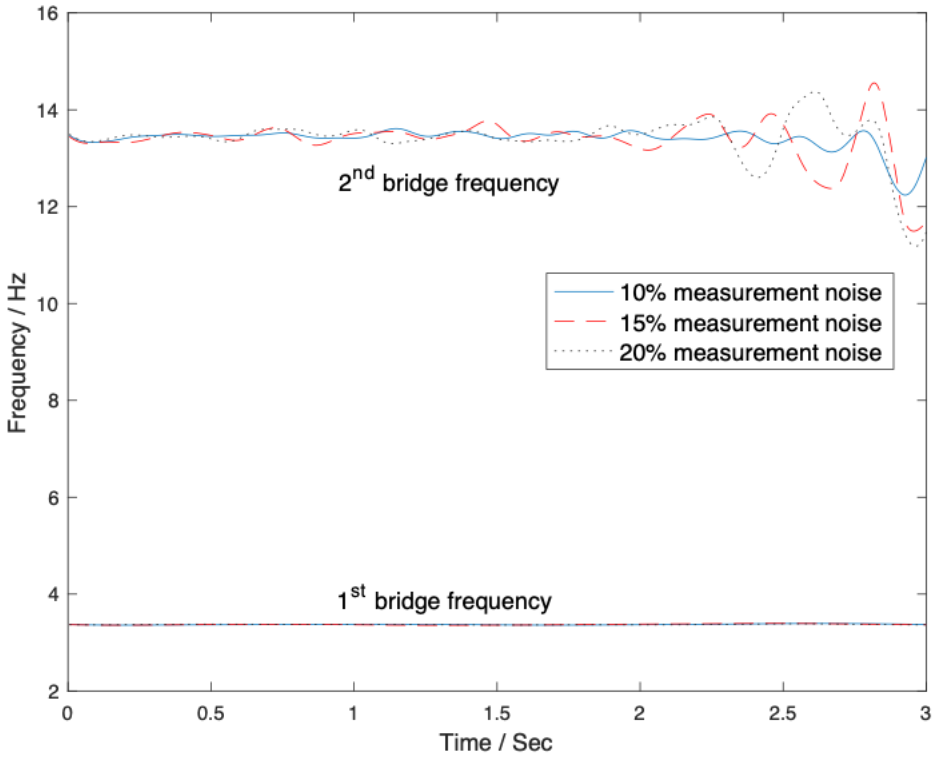

Figure 9 Estimated IFs considering different measurement noise

4.2.3 Effect of bridge surface roughness

A Class A bridge road surface roughness[38] as shown in Figure 10 is introduced in the numerical model and the bridge response is calculated. The proposed method is used to extract the IFs of the response and the identified results are given in Figure 11. It can be seen that the bridge surface roughness changes the variation trend of the response and amplifies the variation amplitude. Therefore, for the VBI based bridge health monitoring, the effects of the roughness should be considered carefully. By considering the case when 20% measurement is included, it can be seen that the effect of road surface roughness on the IFs results is more prominent than that of measurement noise.

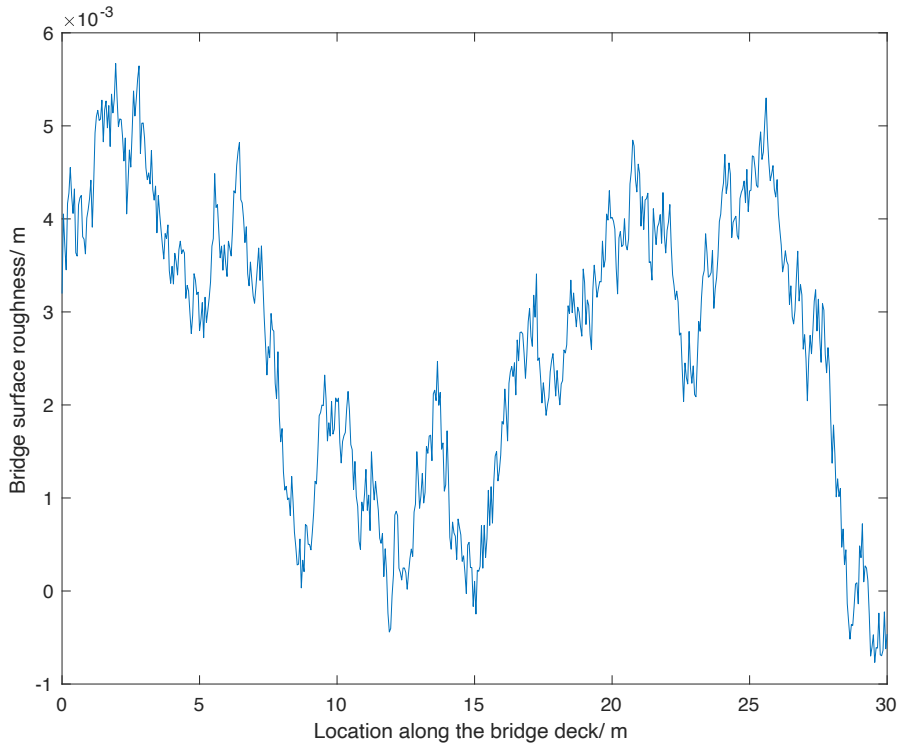

Figure 10 The class A bridge surface roughness

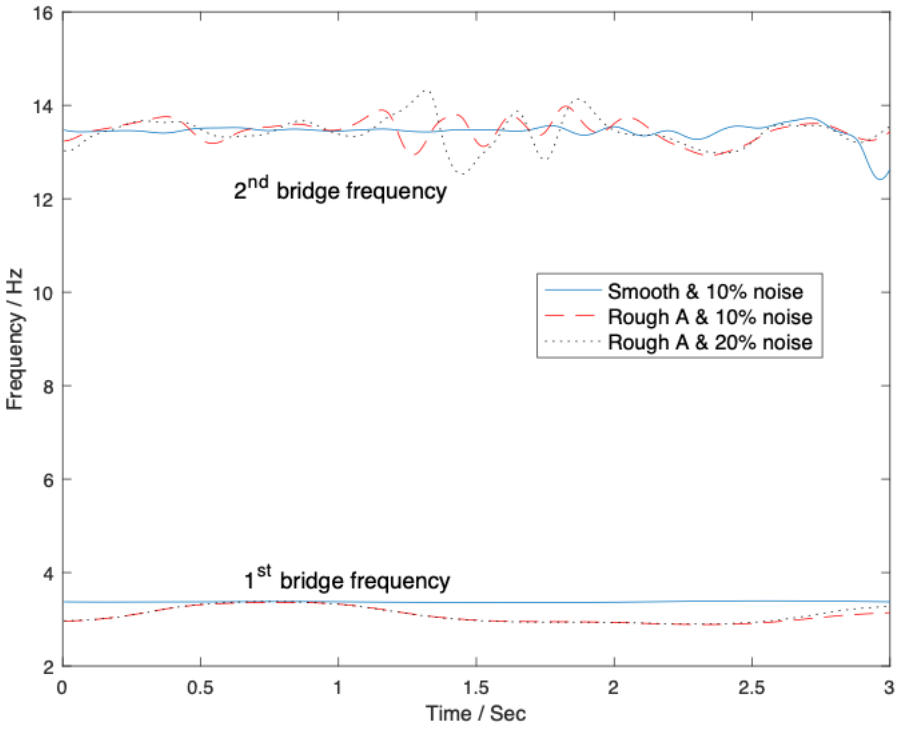

Figure 11 IFs estimation when bridge surface roughness is considered

4.3 Beam with crack damage

A crack is introduced to the bridge model to simulate the bridge structural damage. According to Sinha et al.[39], the crack damage causes a linearly varying decrease in flexural stiffness in its vicinity. The crack is assumed at the 1/3 span of the bridge with the crack level 10% and 20% of the overall bridge

cross-section depth, respectively. Bridge response is analyzed to extract the IFs. From the results as shown in Figure 12, the bridge frequencies decrease due to the crack damage. The results confirmed that the change of the frequency can be used for damage detection. However, the identified IFs do not give information on the damage location.

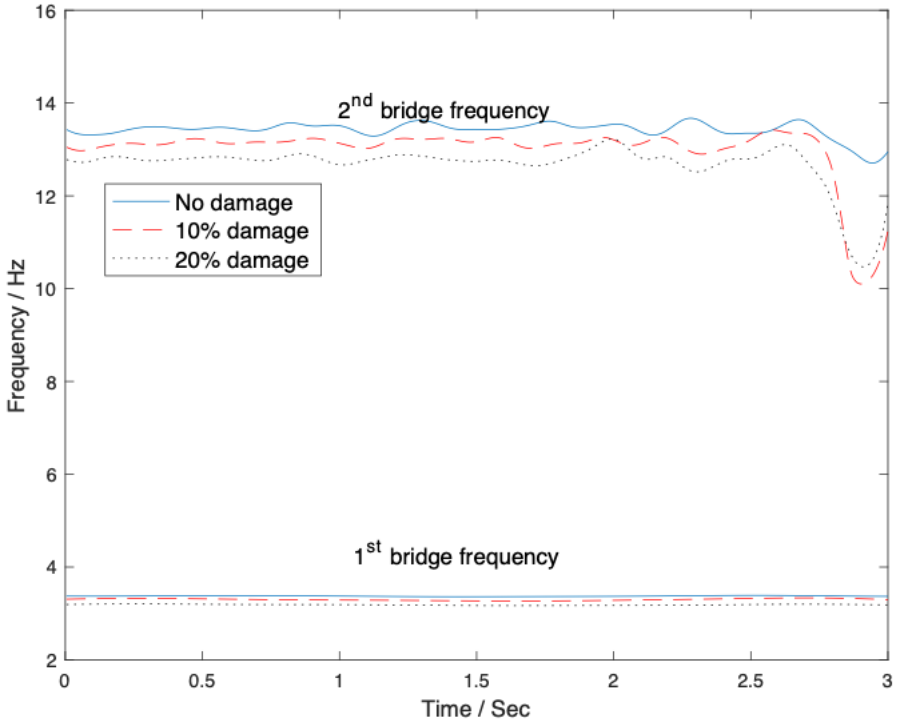

Figure 12 IFs estimation when bridge is damaged

5. IF estimation of the response of an actual bridge

A long-term monitoring system has been installed on a cable-stayed bridge as shown in Figure 13(a). It is a single lane highway bridge with a span of 46m and a width of 5m. The bridge connects the South and North campuses of the Western Sydney University. There are 24 accelerometers installed on the bridge deck, and Figures 13(b) indicates the sensor locations. A data acquisition system continuously records the data from sensors with a sampling rate of 600Hz. Sun et al.[40] conducted modal identification using a series of bridge responses under ambient excitation. The identified first eight modal frequencies are summarized in Table 1.

(a) The cable-stayed bridge

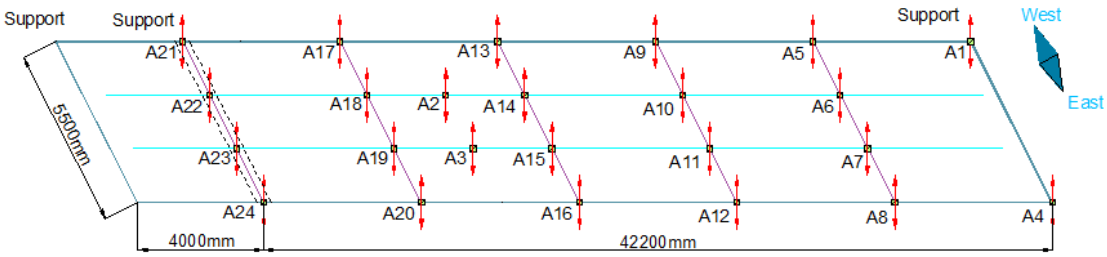

(b) Sensor location

Figure 13 Long-term monitoring of a cable-stayed bridge

The vehicle-induced response of the bridge is studied in this section. Figure 14 shows the acceleration response at sensor A10 and its spectrum when a vehicle is passing over the bridge. Both the wavelet SST and the proposed methods are used to analyze the signal. Figure 15(a) shows the AR power spectrum and the identified boundaries. The identified IFs using the proposed method are shown in Figure 15(b) and the IFs extracted using SST are given in Figure 15(c). For comparison, the estimated IFs results from a recent study[36] is also presented given in Figure 15(d). As Sown in Figure 15(b), the first five IFs are estimated by the proposed method. The associated bridge vibration mode of the IFs is indicated in the figure. The IFs of first vertical bending mode and the coupled Mode 2 and 3 are very similar to the results from SST and reference as shown in Figures 15(c) and (d), respectively. The identified IFs of coupled 6 and 7 mode from three methods are also comparable. Moreover, the results of the proposed method and that from the reference give the time-varying dynamic information related to the coupled Mode 4 and 5. It can also be seen that the proposed method successfully reveals more time-varying characteristics related to the vehicle-induced bridge response than that from the other methods.

Table 1 The identified bridge modal frequencies via modal analysis

Mode number	Frequency (Hz)	Vibration mode
1	2.032	First vertical bending mode of the deck
2	3.548	Double mode that corresponds to the second vertical bending mode
3	3.649	
4	5.584	Third bending mode
5	6.136	A mixture of torsion and bending modes
6	8.044	A mixture of torsion and bending modes
7	8.671	A mixture of the fourth bending mode and torsion
8	11.561	A mixture of the fourth bending mode and torsion

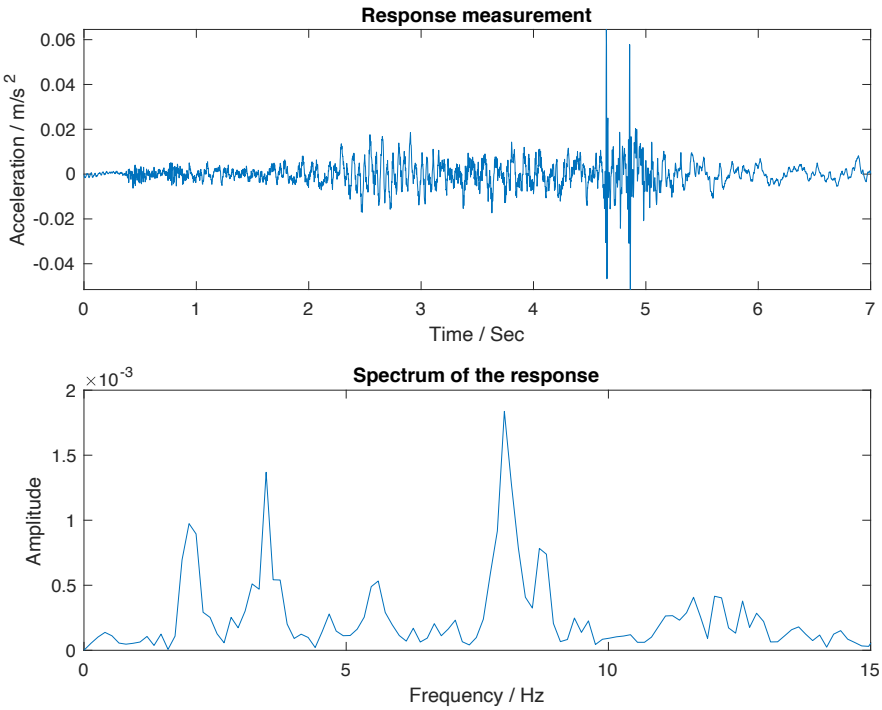

Figure 14 A set of acceleration response and the response spectrum

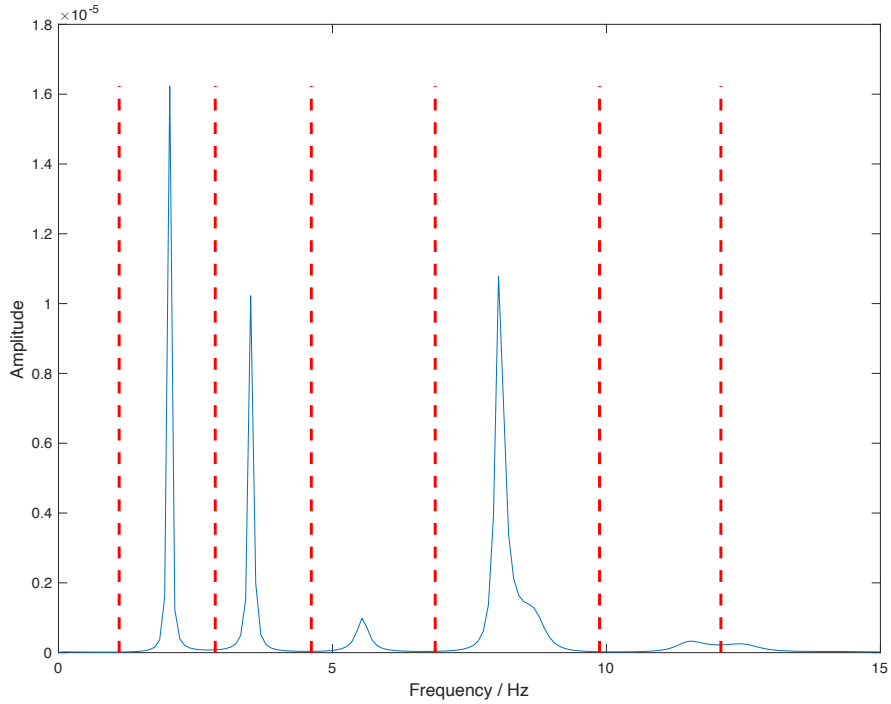

(a) AR spectrum and identified boundaries

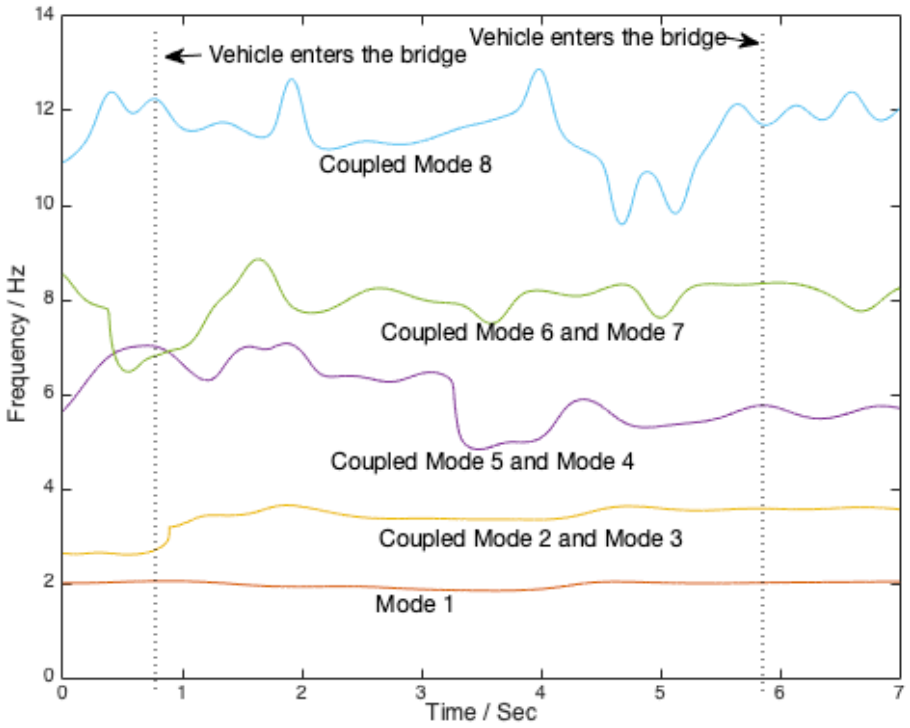

(b) IFs estimation using proposed method

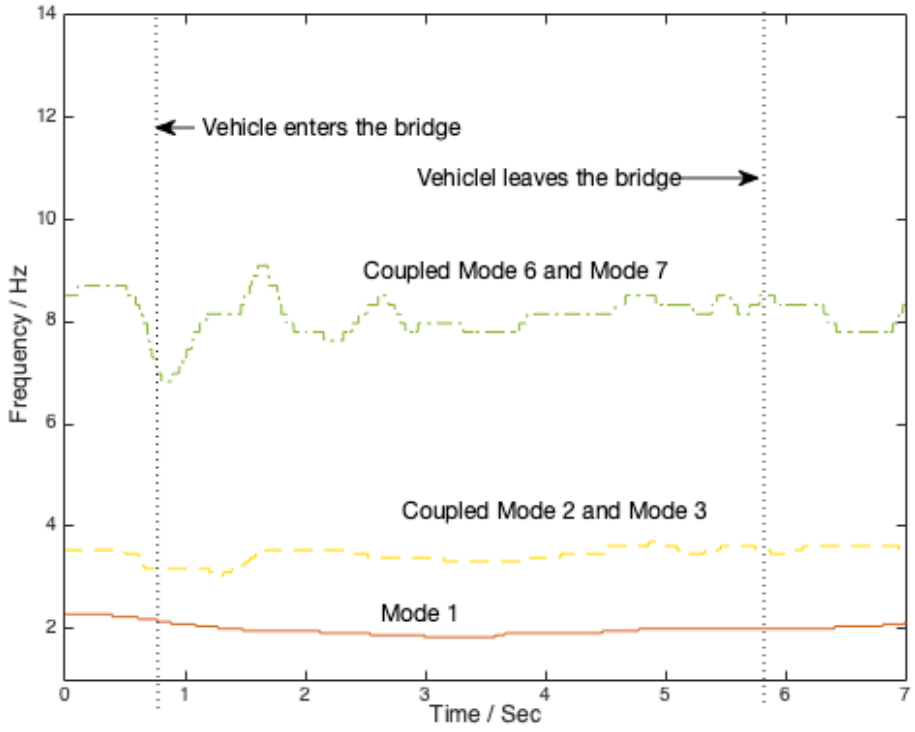

(c) IFs estimation using SST

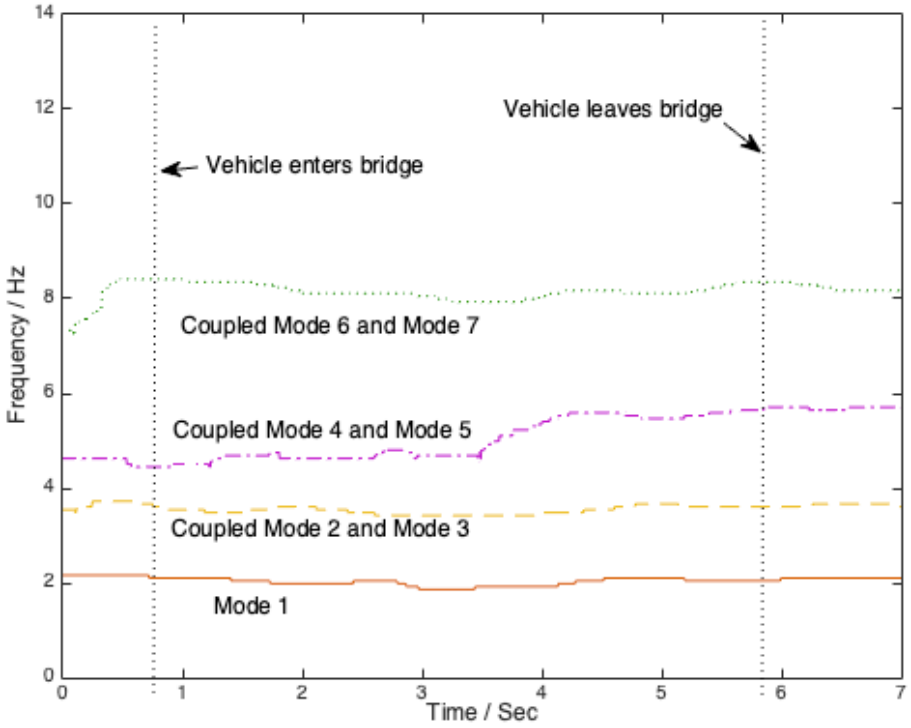

(d) IFs estimation from reference[36]

Figure 15 The estimation of IFs of bridge response

6. Conclusions

The identification of time-varying characteristics of vehicle-induced bridge dynamic response is a complex yet important task. This paper focuses on the vehicle-bridge interaction system and proposed a hybrid method for the analysis of the nonstationary bridge responses. The method combines the improved empirical wavelet transform and a TFR ridge detection technique to extract the IFs. Numerical and experimental are conducted and the results verified the feasibility and effectiveness of the proposed method by comparing with some commonly used methods. The implementation of the proposed method to the response of an in-situ bridge reveals the important time-dependent evolution information of the bridge dynamic characteristics due to the moving operational vehicle load. Further study is needed for practical applications, such as including the 3-D vehicle-bridge interaction model.

Acknowledgements

This research is supported in part by research funding of the National Key Research and Development Projects (2018YFC0809604) and the National Natural Science Foundation of China (U1709207). The financial aid is gratefully acknowledged. DATA61 is greatly acknowledged for the instrumentation of the field bridge for monitoring.

References

1. Kim, J.H., Lynch, J.P., 2013. Experimental analysis of vehicle-bridge interaction using a wireless monitoring system and a two-stage system identification technique. *Mechanical Systems and Signal Processing*, **28**:3-19.
2. Elhattab, A., Uddin, N., O'Brien E.J., 2016. Drive-by bridge damage monitoring using bridge

displacement profile difference. *Journal of Civil Structural Health Monitoring*, **6**(5): 839-850.

3. Yang, Y.B., Yang, J.P., 2017. State-of-the-art review on modal identification and damage detection of bridges by moving test vehicles. I*nternational Journal of Structural Stability and Dynamics*, **18**(2):1850025.
4. Chen, Z., Xie, Z., Zhang, J., 2018. Measurement of Vehicle-Bridge-Interaction force using dynamic tire pressure monitoring, *Mechanical Systems and Signal Processing*, **104**: 370-383.
5. Zhu, X.Q., Law, S.S., 2015. Structural health monitoring based on vehicle-bridge interaction: accomplishments and challenges. *Advances in Structural Engineering*, **18**(12): 1999-2015.
6. Xiao, F., Chen, G.S., Hulsey, J.L., Zatar, W., 2017. Characterization of non-stationary properties of vehicle–bridge response for structural health monitoring. *Advances in Mechanical Engineering*, **9**:1687814017699141.
7. Li, J.Z., Su, M.B., Fan, L.C., 2003. Natural frequency of railway girder bridges under vehicle loads. *Journal of Bridge Engineering ASCE*, **8**(4):199-203.
8. Kim, C.Y., Jung, D.S., Kim, N.S., Kwon, S.D., Feng, M.Q., 2003. Effect of vehicle weight on natural frequencies of bridges measured from traffic-induced vibration. *Earthquake Engineering and Engineering Vibration*, **2**(1):109-115.
9. Chang, K.C., Kim, C.W., Borjigin, S., 2014. Variability in bridge frequency induced by a parked vehicle. *Smart Structures and Systems*, **13**(5):755-773.
10. Cantero, D., McGetrick, P., Kim, C.W., O'Brien, E.J., 2019. Experimental monitoring of bridge frequency evolution during the passage of vehicles with different suspension properties. *Engineering Structures*, **187**:209-219.
11. Su, W.C., Liu, C.Y., Huang, C.S., 2014, Identification of Instantaneous modal parameter of time-varying systems via a wavelet-based approach and its application. Computer-Aided Civil and Infrastructure Engineering, **29**(4):279-298.
12. Huang, N.E., Shen, Z., Long, S.R., Wu, M.C., Shih, H.H., Zheng, Q.A., Yen, N.C., Tung, C.C., Liu, H.H., 1998. The empirical mode decomposition and the Hilbert spectrum for nonlinear and nonstationary time series analysis. *Proceedings of the Royal Society of Landon, Series A*, **454**: 903-955.
13. Wang, Z.C., Ren, W.X., Chen, G.D., 2018. Time-frequency analysis and applications in time-varying/nonlinear structural systems: a state-of-the-art review. *Advances in Structural Engineering*, **21**(10): 1562-1584.
14. Yang, Y., Peng, Z.K., Zhang, W.M., Meng G., 2019. Parameterised time-frequency analysis methods and their engineering applications: a review of recent advances. *Mechanical Systems and Signal Processing*, **119**:182-221.
15. Daubechies, I., Lu, J., Wu, H.T., 2011. Synchrosqueezed Wavelet Transforms: an empirical mode decomposition-like tool. *Applied and Computational Harmonic Analysis*, **30**(2):243-261.
16. Thakur, G., Brevdo, E., Fučkar, N.S., Wu, H.T., 2013. The Synchrosqueezing algorithm for time-varying spectral analysis: robustness properties and new paleoclimate applications. *Signal Processing*, **93**:1079-1094.
17. Luo, J.S., Zhang S.H., Zhong, M.G., Lin, Z.S., 2016. Order spectrum analysis for bearing fault detection via joint application of synchrosqueezing transform and multiscale chirplet path pursuit. *Shock and Vibration*, **2016**: 2976389.
18. Jiang, Q.T., Suter, B.W., 2017. Instantaneous frequency estimation based on synchrosqueezing wavelet transform. *Signal Processing*, **138**: 167-181.
19. Gilles, J., 2013. Empirical wavelet transform. *IEEE Transactions on Signal Processing*,

61(16):3999-4010.

20. Chen, J.L., Pan, J., Li Z.P., Zi, Y.Y., Chen, X.F., 2016. Generator bearing fault diagnosis for wind turbine via empirical wavelet transform using measured vibration signals. *Renewable Energy*, **89**:80-92.
21. Hu, Y., Tu, X.T., Li, F.C., Li, H.G., Meng, G., 2017. An adaptive and tacholess order analysis method based on enhanced empirical wavelet transform for fault detection of bearings with varying speeds. *Journal of Sound and Vibration*, **409**:241-255.
22. Qiao, Z.C., Liu, Y.Q., Liao, Y.Y., 2020. An improved method of EWT and its application in rolling bearings fault diagnosis. *Shock and Vibration*, **2020**: 4973941.
23. Kedadouche M., Thomas, M., Tahan, A., 2016. A comparative study between empirical wavelet transforms and empirical mode decomposition methods: application to bearing defect diagnosis. *Mechanical Systems and Signal Processing*, **81**:88-107.
24. Amezquita-Sanchez, J.P., Park, H.S., Adeli, H., 2017. A novel methodology for modal parameters identification of large smart structures using MUSIC, empirical wavelet transform, and Hilbert transform. *Engineering Structures*, **147**: 148-159.
25. Xia, Y.X., Zhou, Y.L., 2019. Mono-component feature extraction for condition assessment in civil structures using empirical wavelet transform. *Sensors*, **19**(19): 4280.
26. Xin, Y., Hao, H., Li, J., 2019. Operational modal identification of structures based on improved empirical wavelet transform. Structural Control and Health Monitoring, **26**(3): e2323.
27. Xin, Y., Hao, H., Li, J., 2019. Time-varying system identification by enhanced empirical wavelet transform based on synchroextracting transform. *Engineering Structures*, 196: 109313.
28. Zhu, X.Q., Law, S.S., Huang, L., Zhu, S.Y., 2018. Damage identification of supporting structures with a moving sensory system. *Journal of Sound and Vibration*, **415**:111-127.
29. Daubechies, I., 1992. Ten Lectures on Wavelets. Society for Industrial and Applied Mathematics, CBMS-NSF Regional Conference Series in Applied Mathematics.
30. Percival, D.B. and Walden, A.T., 1993. Spectral analysis for physical applications: multitaper and conventional univariate techniques. Cambridge, UK: Cambridge University Press.
31. Ljung, L., 1999. System identification: theory for the user. Second Edition, Upper Saddle River, New Jersey: Prentice-Hall PTR.
32. Iatsenko, D., McClintock, P.V.E., Stefanovska, A., 2016. Extraction of instantaneous frequencies from ridges in time-frequency representations of signals. *Signal Processing*, **125**:290-303.
33. Feng, Z., Liang, M., Chu, F., 2013. Recent advances in time-frequency analysis methods for machinery fault diagnosis: a review with application examples. *Mechanical Systems and Signal Processing*, **38**(1):165-205.
34. Huang, H., Baddour, N., Liang, M., 2019. Multiple time-frequency curve extraction Matlab code and its application to automatic bearing fault diagnosis under time-varying speed conditions. *MethodsX*, **6**:1415-1432.
35. Yang Y.B., Cheng M.C., Chang, K.C., 2013. Frequency variation in vehicle–bridge interaction systems. *International Journal of Structural Stability and Dynamics,* **13**(2): 1350019.
36. Li J.T., Zhu X.Q., Law S.S., Samali B., 2020. Time-varying characteristics of bridges under the passage of vehicles using synchroextracting transform. *Mechanical System and Signal Processing,* **140**:106727.
37. Yang, Y.B., Lin, C.W., Yau. J.D., 2004. Extracting bridge frequencies from the dynamic response of

a passing vehicle. *Journal of Sound and Vibration*, **272**:471-493. doi:10.1016/S0022-460X(03)00378-X

38. ISO-8608, 1995. Mechanical vibration-Road surface profiles-Reporting of measured data. International Organization for Standardization (ISO), Geneva, Switzerland.
39. Sinha, J.K., Friswell, M.I., Edwards, S., 2002. Simplified models for the location of cracks in beam structures using measured vibration data. Journal of Sound and Vibration, **251**(1):13–38.
40. Sun, M., Alamdari, M.M., Kalhori, H., 2017. Automated Operational Modal Analysis of a Cable-Stayed Bridge. *Journal of Bridge Engineering*, **22**(12): 05017012.